Magnetization properties and vortex phase diagram of Cu$_x$TiSe$_2$ single crystals

P. Husaníková,[1,2] J. Fedor,[2] J. Dérer,[2] J. Šoltýs,[2] V. Cambel,[2] M. Iavarone,[3] S. J. May,[4] and G. Karapetrov[1,*]

[1]*Department of Physics, Drexel University, 3141 Chestnut Street, Philadelphia, Pennsylvania 19104, USA*
[2]*Institute of Electrical Engineering, Slovak Academy of Sciences, Dúbravská cesta 9, SK-841 04 Bratislava, Slovakia*
[3]*Department of Physics, Temple University, Philadelphia, Pennsylvania 19122, USA*
[4]*Department Materials Science and Engineering, Drexel University, 3141 Chestnut Street, Philadelphia, Pennsylvania 19104, USA*

We have investigated the magnetization properties and flux dynamics of superconducting Cu$_x$TiSe$_2$ single crystals within a wide range of copper concentrations. We find that the superconducting anisotropy is low and independent on copper concentration ($\gamma \sim 1.7$), except in the case of strongly underdoped samples ($x \leqslant 0.06$) that show a gradual increase in anisotropy to $\gamma \sim 1.9$. The vortex phase diagram in this material is characterized by a broad region of vortex liquid phase that is unusual for such a low-T_c superconductor with low anisotropy. Below the irreversibility line the vortex solid state supports relatively low critical current densities as compared to the depairing current limit ($J_c/J_0 \sim 10^{-7}$). All this points out that local fluctuations in copper concentration have little effect on bulk pinning properties in this system.

$1T - \mathrm{TiSe}_2$, a quasi-2D layered material with a trigonal symmetry, has been studied for over 30 years due to the unconventional nature of its charge density wave (CDW) state.[1–7] Recently, the superconductivity was discovered in this system below 4.15 K by intercalating copper between the van der Waals–coupled Se-Ti-Se trilayers.[8] Subsequently, superconductivity was also induced by palladium intercalation,[9] as well as by hydrostatic pressure in pristine $1T - \mathrm{TiSe}_2$.[10] Despite the low superconducting critical temperature T_c, the material has attracted significant attention due to the peculiar nature of the emergent superconductivity from a semimetallic state above T_c, as well as the coexistence of the superconductivity with the chiral CDW state.[11–13] The initial studies probing the superconducting phase in Cu$_x$TiSe$_2$ have yielded diverging results ranging from multiple superconducting energy gaps,[14] to weakly coupled superconductivity and the presence of spin fluctuations.[15] ARPES measurements near the superconducting transition have shown d-like character of the emergent density of states near the L point of the Brillouin zone at Cu concentrations $x > 0.04$ with competing nature of CDW and superconducting order parameters.[16] On the other hand, detailed specific heat measurements of superconducting Cu$_x$TiSe$_2$ have shown that the system behaves as a conventional s-wave superconductor with $2\Delta/k_B T_c \sim 3.7$.[17,18] It is remarkable that for such a simple compound as TiSe$_2$, there are diverging explanations about the origin of the emergent superconductivity. The phase diagram of the Cu-doped TiSe$_2$ is similar to the one of high-temperature superconductors, pnictides, and heavy fermions, in that the superconducting phase at the specific doping interval coexists with other correlated electron states (charge or spin ordering). Considering the relatively simple lattice structure of the parent compound $1T - \mathrm{TiSe}_2$, the system should be suitable for detailed studies of emergent superconductivity and the evolution of competing order parameters, CDW and superconductivity.

Besides the intriguing electronic properties very little is known about the Abrikosov vortex configurations in this superconductor. The static and dynamic behavior of the vortex lattice, anisotropy of the superconducting order parameters

and vortex lattice phase diagram could provide further insight into the superconducting state in Cu$_x$TiSe$_2$ and the specific role that copper plays in facilitating superconductivity. In this work we study anisotropic superconducting properties of Cu$_x$TiSe$_2$ single crystals via bulk magnetization measurements for a range of copper concentrations spanning from the highly underdoped regime to the overdoped one. We establish fundamental superconducting parameters of this system such as upper critical field, coherence length, and superconducting anisotropy. We establish the vortex phase diagram of Cu$_x$TiSe$_2$ and we find that the reversibility region is unexpectedly broad for an extended range of Cu doping values. Despite the atomic disorder created by intercalated copper atoms, we observe very low bulk pinning in this material even far from T_c. This points to a uniform amplitude of the superconducting order parameter across the sample and vortex liquid-like behavior of the vortex lattice.

Cu$_x$TiSe$_2$ single crystals were grown by means of iodine vapor transport method in evacuated silica ampoules in a gradient furnace with the lower temperature part set to 720°C and the temperature gradient of 80°C/m. An average crystal size was on the order of few mm^2 with thickness of several tens of micrometers. Energy dispersive x-ray spectroscopy (EDS) was used to establish the quantitative elemental content of the crystals. The selected single crystals were analyzed for spatial uniformity of copper concentration by performing EDS analysis at several points across the sample. The crystals with good spatial uniformity of copper and sharp superconducting transition were selected for detailed studies of magnetization properties. The magnetization measurements were conducted within few weeks from the single crystal growth as copper tends to migrate with time. Magnetization measurements were performed in a vibrating sample magnetometer of PPMS, as well as SQUID magnetometer (Quantum Design PPMS w/VSM option and MPMS, respectively).

We studied Cu$_x$TiSe$_2$ single crystals with Cu concentrations of $x = 0.058$, 0.062, 0.067, 0.085, and 0.090 and these cover the range from electron underdoped ($x < 0.08$) to overdoped ($x > 0.08$) regimes. At normal pressure the superconductivity
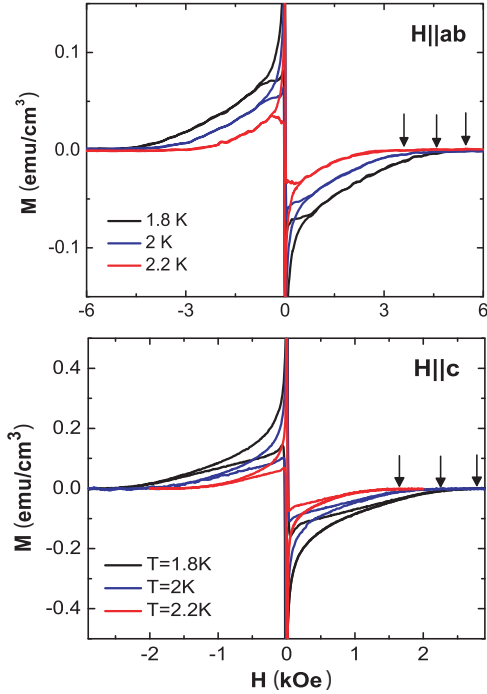
FIG. 1. (Color online) Magnetization hysteresis loops for Cu$_{0.058}$TiSe$_2$ sample for $H \parallel ab$ (top) and $H \parallel c$ (bottom) at different temperatures. The arrows indicate the transitions from superconducting to normal state, defining H_{c2} points.
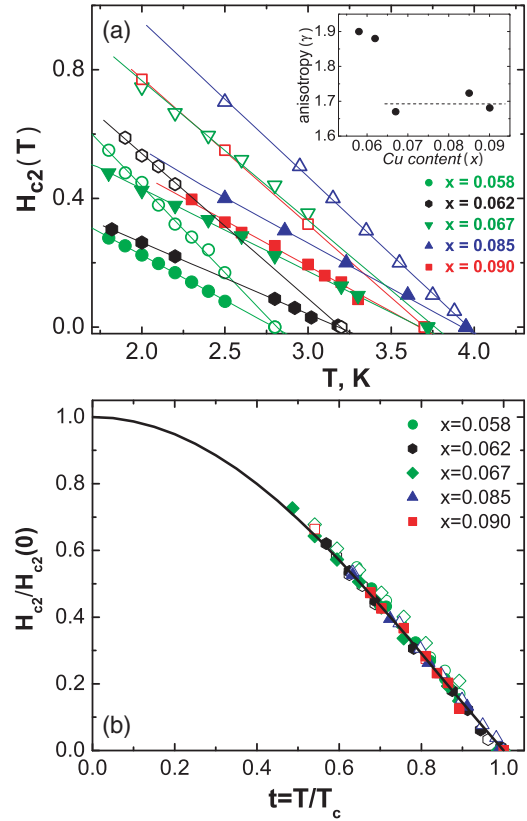

FIG. 2. (Color online) (a) Temperature dependence of the upper critical field H_{c2} determined from magnetization measurements for Cu$_x$TiSe$_2$ samples with five different copper concentrations. Open symbols are for $H \parallel c$ and filled symbols are for $H \parallel ab$. The inset shows the values of the superconducting anisotropy $\gamma = H_{c2}^{ab}(0)/H_{c2}^c(0)$ for different copper concentrations x. (b) Normalized upper critical field dependence on the reduced temperature for all the samples in (a) with both directions of the applied field. The full line is a fit to Eq. (2).

in Cu$_x$TiSe$_2$ emerges at Cu doping of around $x = 0.04$, reaching the maximum critical temperature of 4.15 K at $x = 0.08$. For copper concentrations beyond $x = 0.08$ the T_c starts to gradually decrease.[8] Figure 1 shows the representative magnetization loops for Cu$_{0.058}$TiSe$_2$ for magnetic field applied along the crystallographic planes ($H \parallel ab$) and perpendicular to the planes ($H \parallel c$) from which the upper critical fields were extracted. The hysteresis curves for all samples are characterized by large reversible regions of the magnetization at higher applied fields that can be assigned to the magnetization of the Abrikosov vortex lattice.[19] The irreversibility in magnetization curves observed at lower fields represents the effect of vortex pinning.

From the magnetization curves we extracted the temperature dependence of the upper critical field H_{c2} along the two primary axes, perpendicular and parallel to the crystal planes, as shown in Fig. 2(a). The linear dependence of the $H_{c2}(T)$ near T_c is evident for all copper concentrations. The values of $H_{c2}(0)$ were extracted from the data in Fig. 2(a) using Werthamer-Helfand-Hohenberg (WHH) formula[20]

$$H_{c2}(0) = -0.693 T_c \left(\frac{dH_{c2}}{dT} \right)_{T_c} . \tag{1}$$

This step assumes that the Cu$_x$TiSe$_2$ is an *s*-wave BCS superconductor, which is in accordance to recent results.[18] The data from all samples follow the empirical formula:

$$\frac{H_{c2}(t)}{H_{c2}(0)} = (1 - t^2)(1 - at^2) \tag{2}$$

with parameter $a = 0.3$ that corresponds to approximate WHH behavior of Eq. (1) [i.e., $H_{c2}(0) = 0.7 T_c H_{c2}'(T_c)$], as shown

in Fig. 2(b). The perfect scaling of the data for all copper concentrations signifies that the pair-breaking mechanism of the magnetic field does not depend on the doping level, i.e., it does not depend on the amplitude of the underlying CDW state.

As expected, the $H_{c2}(0)$ varies with Cu concentration x, closely following the $T_c(x)$ profile (Fig. 3). At close-to-optimal doping level ($x = 0.085$) we reach the maximum $H_{c2}^c(0) = 0.76$ T and $H_{c2}^{ab}(0) = 1.31$ T. Using the anisotropic Ginzburg-Landau formulas:[21]

$$H_{c2}^c(0) = \frac{\Phi_0}{2\pi \xi_{ab}^2(0)} \quad ; \quad H_{c2}^{ab}(0) = \frac{\Phi_0}{2\pi \xi_{ab}(0)\xi_c(0)}$$

the superconducting coherence length along the *c* axis $\xi_c(0)$ and in the *ab* plane $\xi_{ab}(0)$ were obtained (here $\Phi_0 = 2.07 \times 10^7$ G cm^2 is the flux quantum). Close to optimally doped sample with $x = 0.085$ shows $\xi_{ab}(0) = 20.5$ nm and $\xi_c(0) = 11.9$ nm. The anisotropy of the upper critical field, $\gamma = H_{c2}^{ab}(0)/H_{c2}^c(0)$, was found to be 1.7 for $x \geqslant 0.067$ and independent on the copper concentration. However, in the highly underdoped regime we found an increase of the anisotropy to $\gamma \sim 1.9$ (inset of Fig. 2). It is interesting to note that compared to other superconducting transition metal
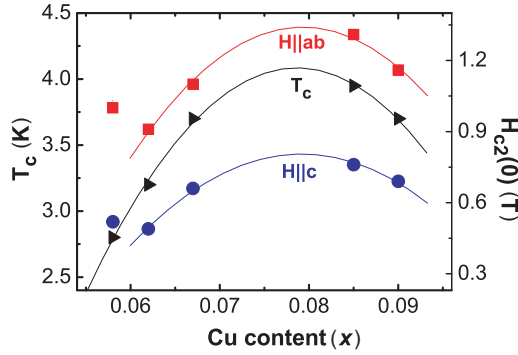
FIG. 3. (Color online) Dependence of the upper critical fields and superconducting transition temperature on the Cu concentration x in $Cu_x TiSe_2$.

dichalcogenides such as 2H-NbS$_2$,[22] 2H-NbSe$_2$,[23,24] Na$_x$TaS$_2$,[25] and 2H-TaSe$_2$,[26] Cu$_x$TiSe$_2$ has the lowest anisotropy of the upper critical field coinciding to one observed in K$_{0.8}$Fe$_2$Se$_2$ superconductor.[27] The values of $H_{c2}(0)$ obtained in the slightly underdoped case ($x = 0.07$) that were reported earlier in Ref. 28 are consistent with our dome-like dependence in Fig. 3.

The physical origin of the deviation in the upper critical field and anisotropy in highly underdoped samples may be due to the confluence of higher electronic anisotropy with lack of available electronic states to form Cooper pairs. The CDW amplitude is strong in the underdoped regime and CDW order parameter competes with superconductivity.[16] For similar Cu concentrations ($x = 0.055$) an unusual behavior of magnetoresistance has been reported recently.[29] Moreover, Kusmartseva et al.[10] observed a sizable suppression of the exponent n in the temperature-dependent resistance $R(T) = R_0 + AT_n$ around the critical pressure of $\sim$3 GPa. This deviation was attributed to quantum fluctuations in the vicinity of the CDW quantum critical point. Similarly, Zaberchik et al.[14] observed a deviation from BCS model in a temperature dependence of a superfluid density for lower copper concentrations in their muon-spin rotation experiments. It is quite possible that at lower Cu concentrations the amplitude of the CDW remains strong despite the presence of the superconducting order parameter, causing an increase of the superconducting anisotropy and decrease of available electronic states participating in superconducting pairing.

Next, we examine in detail the vortex states in Cu$_x$TiSe$_2$ using DC magnetization hysteresis measurements. The bulk superconducting critical current densities are determined from the irreversible part of magnetization loops using the Bean model.[30] For $H \parallel c$, the correspondence between J_c and the width of the magnetization loop is given by the isotropic Bean model,[30] whereas for $H \perp c$ we apply the anisotropic Bean model[31] that takes into account the difference in the superconducting critical current flowing along and perpendicular to the crystal planes. At fields of several hundred Oersteds we can assume that the surface and geometrical barriers do not significantly contribute to the irreversibility in our samples. We use well established expressions for critical current densities in anisotropic superconductors with slab geometry.[31] For $H \parallel c$, in the case of a rectangular shape of
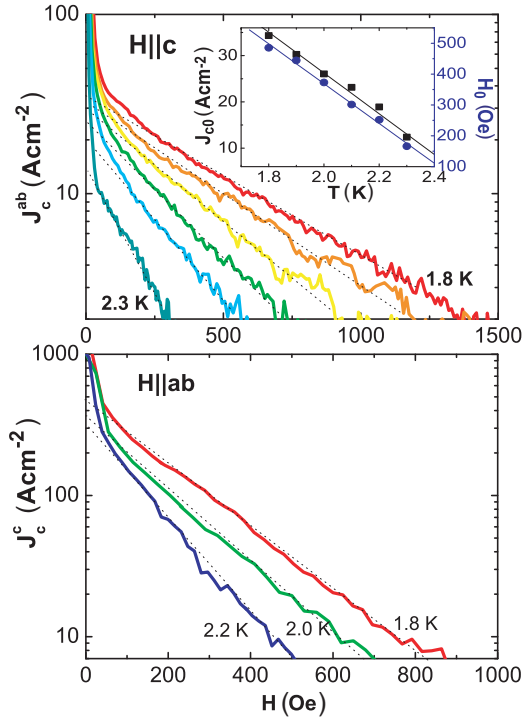

FIG. 4. (Color online) Magnetic field dependence of the superconducting critical current density in Cu$_{0.058}$TiSe$_2$ for applied field $H \parallel c$ at $T = 1.8$, 1.9, 2.0, 2.1, 2.2, and 2.3 K (upper panel) and for $H \parallel ab$ at $T = 1.8$, 2.0, and 2.2 K (lower panel). The curves were fit with Eq. (3) and temperature dependence of parameters J_{c0} and H_0 is shown in the inset.

crystal with $b > a > c$ (b, a, and c are the length, width, and thickness of the sample) the in-plane critical current density is given by[31] $J_c^{ab}(H) = \frac{20\Delta M(H)}{a(1-a/3b)}$, where a, b are the dimensions in cm and ΔM is a difference between the magnetization for decreasing and increasing branch of magnetization loop in emu/cm^3. For magnetic field applied along the ab plane, there are two contributions to the supercurrent—parallel to the Ti-Se layers, J_c^{ab}, and perpendicular to the Ti-Se layers, J_c^c. In the limit $a, b \gg c \frac{J_c^{ab}}{3J_c^c}$, the former is given by $J_c^c = \frac{20\Delta M(H)}{c}$. An example of magnetic field dependence of J_c^c and J_c^{ab} for the sample with $x = 0.058$ are shown in Fig. 4. We observe an exponential dependence that can be expressed using

$$J_c(H,T) = J_{c0}(T)\exp(-H/H_0(T)). \qquad (3)$$

Extracted values of $J_{c0}(T)$ and $H_0(T)$ have a linear temperature dependence shown in the inset of Fig. 4. Similar exponential field dependence of the critical current density was observed in the rest of the samples with different Cu concentrations. Microscopic examination of the samples by scanning tunneling microscopy did not reveal defects on the length scale of the coherence length. The only defects present in the system could be due to Ti interstitials[32] or fluctuation of copper content on a microscopic scale. Since the average distance between the Cu atoms is well below the superconducting coherence length, the intrinsic vortex pinning should be of collective nature[33] caused by the random local fluctuations of the Cu dopant concentration or atomic Ti interstitials.[32]
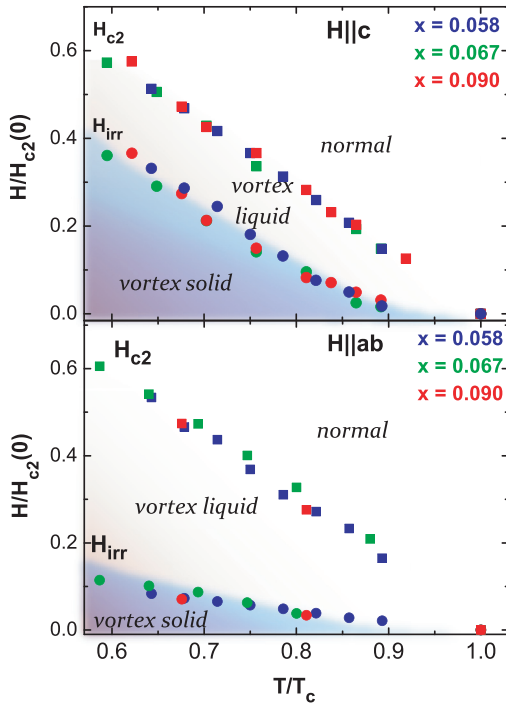
FIG. 5. (Color online) Vortex phase diagram of Cu_xTiSe_2 for magnetic field applied $H \parallel c$ (upper panel) and $\parallel ab$ (lower panel).

The relatively large reversible part of the magnetization curve $M(H)$ spanning up to H_{c2} signifies the presence of a vortex liquid phase. The boundary between vortex solid and liquid phases, the irreversibility field H_{irr}, was inferred from the magnetization hysteresis loops as a field at which upper and lower magnetization branches merge. As an onset criterium of reversibility we used the value of $\Delta m \leqslant 5 \times 10^{-7}$ emu. A vortex phase diagram for samples with different copper concentrations is shown in Fig. 5.

The perfect scaling of the $H_{c2}(T)$ and $H_{irr}(T)$ with T_c is further evidence that the underlying nature of the vortex dynamics in samples with different Cu concentration is the same. It is remarkable to notice that the reversible region of the vortex liquid phase is so broad for such a low-T_c material with relatively low superconducting anisotropy. Normally, the broad vortex liquid region in the phase diagram is associated with the existence of thermal fluctuations, a perfect example of which are the high temperature superconductors. The irrelevance of thermal fluctuations in our system can be inferred from the estimate of the Ginzburg number $G \sim 3 \times 10^{-6}$, a

value much smaller than the one found in high-T_c materials ($G \geqslant 10^{-3}$).[34] The estimate of the ratio of the critical current density to the depairing current density $J_c(H,T)/J_0$, provides a measure of the magnitude of the quenched disorder (where depairing current $J_0 = \frac{4H_c}{3\sqrt{6}\mu_0\lambda}$, λ is London penetration depth, H_c is thermodynamical critical field, and μ_0 is permeability of vacuum). In Cu_xTiSe_2 this ratio is found to be $\sim 4 \times 10^{-7}$, which is much smaller than the one found typically in single crystal of low-T_c dichalcogenide superconductors such as $NbSe_2$ ($\sim 10^{-3}$). From this we can conclude that the broad area of the vortex liquid phase in the phase diagram is evidence of high copper dopant spatial homogeneity that results in vanishing quenched disorder. It is possible that additional mechanisms could play a role in reducing the shear modulus of the vortex lattice, but this issue would need to be addressed through a combination of microscopic measurements of the local density of states of the individual vortex line and vortex lattice configurations.[35]

In conclusion, we have investigated the magnetization properties and flux dynamics of Cu_xTiSe_2 single crystals in a wide range of copper concentrations. We find that the superconducting anisotropy is independent on Cu concentration except in the case of strongly underdoped samples that show a gradual increase in anisotropy. We establish the vortex phase diagram in this material. We find a broad, doping-independent region of vortex liquid phase that is unusual for such low-T_c superconductor with low anisotropy. Deep in the vortex solid phase the pinning remains very weak compared to other dichalcogenide superconductors. This leads us to believe that fluctuations in copper concentration on a nanometer scale have little effect on the pinning potential landscape.

*goran@drexel.edu

[1]J. Wilson, Solid State Commun. **22**, 551 (1977).

[2]F. J. Di Salvo, D. E. Moncton, and J. V. Waszczak, Phys. Rev. B **14**, 4321 (1976).

[3]K. Rossnagel, L. Kipp, and M. Skibowski, Phys. Rev. B **65**, 235101 (2002).

[4]T. E. Kidd, T. Miller, M. Y. Chou, and T.-C. Chiang, Phys. Rev. Lett. **88**, 226402 (2002).

[5]C. Monney, E. F. Schwier, M. G. Garnier, N. Mariotti, C. Didiot, H. Beck, P. Aebi, H. Cercellier, J. Marcus, C. Battaglia *et al.*, Phys. Rev. B **81**, 155104 (2010).

[6]J. van Wezel, P. Nahai-Williamson, and S. S. Saxena, Phys. Rev. B **83**, 024502 (2011).

[7]K. Rossnagel, J. Phys.: Condens. Matter **23**, 213001 (2011).

[8] E. Morosan, H. W. Zandbergen, B. S. Dennis, J. W. G. Bos, Y. Onose, T. Klimczuk, A. P. Ramirez, N. P. Ong, and R. J. Cava, Nat. Phys. **2**, 544 (2006).

[9] E. Morosan, K. E. Wagner, L. L. Zhao, Y. Hor, A. J. Williams, J. Tao, Y. Zhu, and R. J. Cava, Phys. Rev. B **81**, 094524 (2010).

[10] A. F. Kusmartseva, B. Sipos, H. Berger, L. Forro, and E. Tutis, Phys. Rev. Lett. **103**, 236401 (2009).

[11] M. Iavarone, R. Di Capua, X. Zhang, M. Golalikhani, S. A. Moore, and G. Karapetrov, Phys. Rev. B **85**, 155103 (2012).

[12] J. P. Castellan, S. Rosenkranz, R. Osborn, Q. Li, K. E. Gray, X. Luo, U. Welp, G. Karapetrov, J. P. C. Ruff, and J. van Wezel, Phys. Rev. Lett. **110**, 196404 (2013).

[13] J. Ishioka, Y. H. Liu, K. Shimatake, T. Kurosawa, K. Ichimura, Y. Toda, M. Oda, and S. Tanda, Phys. Rev. Lett. **105**, 176401 (2010).

[14] M. Zaberchik, K. Chashka, L. Patlgan, A. Maniv, C. Baines, P. King, and A. Kanigel, Phys. Rev. B **81**, 220505 (2010).

[15] A. D. Hillier, P. Manuel, D. T. Adroja, J. W. Taylor, A. K. Azad, and J. T. S. Irvine, Phys. Rev. B **81**, 092507 (2010).

[16] D. Qian, D. Hsieh, L. Wray, E. Morosan, N. L. Wang, Y. Xia, R. J. Cava, and M. Z. Hasan, Phys. Rev. Lett. **98**, 117007 (2007).

[17] S. Y. Li, L. Taillefer, G. Wu, and X. H. Chen, Phys. Rev. Lett. **99**, 107001 (2007).

[18] J. Kacmarcik, Z. Pribulova, V. Paluchova, P. Szabo, P. Husanikova, G. Karapetrov, and P. Samuely, Phys. Rev. B **88**, 020507 (2013).

[19] S. Senoussi, J. Phys. III **2**, 1041 (1992).

[20] N. R. Werthamer, E. Helfand, and P. C. Hohenberg, Phys. Rev. **147**, 295 (1966); E. Helfand and N. R. Werthamer, *ibid*. **147**, 288 (1966).

[21] J. R. Clem, Physica C **162–164**, 1137 (1989).

[22] M. Leroux, P. Rodire, L. Cario, and T. Klein, Physica B **407**, 1813 (2012).

[23] R. C. Morris, R. V. Coleman, and R. Bhandari, Phys. Rev. B **5**, 895 (1972).

[24] D. Sanchez, A. Junod, J. Muller, H. Berger, and F. Levy, Physica B **204**, 167 (1995).

[25] L. Fang, Y. Wang, P. Y. Zou, L. Tang, Z. Xu, H. Chen, C. Dong, L. Shan, and H. H. Wen, Phys. Rev. B **72**, 014534 (2005).

[26] K. Yokota, G. Kurata, T. Matsui, and H. Fukuyama, Physica B **284–288**, 551 (2000).

[27] J. Ge, J. Gutierrez, M. Li, J. Zhang, and V. V. Moshchalkov, Appl. Phys. Lett. **103**, 052602 (2013).

[28] E. Morosan, L. Li, N. P. Ong, and R. J. Cava, Phys. Rev. B **75**, 104505 (2007).

[29] G. Wu, H. X. Yang, L. Zhao, X. G. Luo, T. Wu, G. Y. Wang, and X. H. Chen, Phys. Rev. B **76**, 024513 (2007).

[30] C. Bean, Phys. Rev. Lett. **8**, 250 (1962); Rev. Mod. Phys. **36**, 31 (1964).

[31] E. M. Gyorgy, R. B. van Dover, K. A. Jackson, L. F. Schneemeyer, and J. V. Waszczak, Appl. Phys. Lett. **55**, 283 (1989); V. Moshchalkov, A. Zhukov, L. Leaniuk, V. Kuznetsov, and V. Metlushko, Sov. Phys. Supercond. **2**, 84 (1989).

[32] M. Wiesenmayer, S. Hilgenfeldt, S. Mathias, F. Steeb, T. Rohwer, and M. Bauer, Phys. Rev. B **82**, 035422 (2010).

[33] A. I. Larkin and Y. N. Ovchinnikov, J. Low Temp. Phys. **34**, 409 (1979).

[34] G. Blatter, M. V. Feigelman, V. B. Geshkenbein, A. I. Larkin, and V. M. Vinokur, Rev. Mod. Phys. **66**, 1125 (1994).

[35] M. Iavarone, R. Di Capua, G. Karapetrov, A. E. Koshelev, D. Rosenmann, H. Claus, C. D. Malliakas, M. G. Kanatzidis, T. Nishizaki, and N. Kobayashi, Phys. Rev. B **78**, 174518 (2008).